High selectivity and sensitivity through nanoparticle sensors for cleanroom CO 2 detection

Nanotechnology

High selectivity and sensitivity through nanoparticle sensors for cleanroom CO_2 detection

To cite this article before publication: Manjunatha Channegowda *et al* 2024 *Nanotechnology* in press https://doi.org/10.1088/1361-6528/ad3fbf

High Selectivity and Sensitivity through Nanoparticle Sensors for Cleanroom CO_2 Detection

Manjunatha Channegowda, Arpit Verma[1,2], Igra Arabia[3], Ujwal S Meda[3], Ishpal Rawal[4], Sarevesh Rustagi[5], Bal Chandra Yadav[2], Patrick Dunlop[6], Nikhil Bhalla[6,7] and Vishal Chaudhary[8]

[1]Department of Chemistry, RV College of Engineering, 560059, Bengaluru, India
[2]Department of Physics, Babasaheb Bhimrao Ambedkar University, Lucknow226025, U.P, India
[3]Department of Chemical Engineering, RV College of Engineering, 560059, Bengaluru, India
[4]Department of Physics, Kirori Mal College, University of Delhi, 110007, Delhi, India
[5]Department of Food Technology, School of Applied and Life Sciences, Uttaranchal University, Uttrakhand, 248002, Dehradun, India
[6]Nanotechnology and Integrated Bioengineering Centre (NIBEC), School of Engineering, Ulster University, 2-24 York Street, Belfast, Northern Ireland BT15 1AP, United Kingdom
[7]Healthcare Technology Hub, Ulster University, 2-24 York Street, Belfast, Northern Ireland BT15 1AP, United Kingdom

E-mail: n.bhalla@ulster.ac.uk (Nikhil Bhalla)
[8]Physics Department, Bhagini Nivedita College (BNC), University of Delhi, New Delhi 110043, India

E-mail: drvishal@bn.du.ac.in (V.C.); n.bhalla@ulster.ac.uk (N.B.)

Abstract. Clean room facilities are becoming more popular in both academic and industry settings, including low-and middle-income countries. This has led to an increased demand for cost-effective gas sensors to monitor air quality. Here we have developed a gas sensor using $CoNiO_2$ nanoparticles through combustion method. The sensitivity and selectivity of the sensor towards CO_2 were influenced by the structure of the nanoparticles, which were affected by the reducing agent (biofuels) used during synthesis. Among all reducing agents, urea found to yield highly crystalline and uniformly distributed $CoNiO_2$ nanoparticles, which when developed into sensors showed high sensitivity and selectivity for the detection of CO_2 gas in the presence of common interfering volatile organic compounds observed in cleanroom facilities including ammonia, formaldehyde, acetone, toluene, ethanol, isopropanol and methanol. In addition, the urea-mediated nanoparticle-based sensors exhibited room temperature operation, high stability, prompt response and recovery rates, and excellent reproducibility. Consequently, the synthesis approach to nanoparticle-based, energy efficient and affordable sensors represent a benchmark for CO_2 sensing in cleanroom settings.

Keywords: carbon-dioxide, nanoparticles, clearnroom, gas-sensors

1. Introduction

Perhaps most common in the semiconductor and materials industry, cleanrooms are used in a range of sectors where small airborne particles can lead to adverse effects on the manufacturing process and quality of engineered materials [1, 2]. In addition to particles, cleanroom facilities are specifically designed to control and maintain specific air quality, including temperature, pressure and flow rate. Currently, cleanrooms are categorized into classes based on the level of particle contamination [1], but there is significant requirement for the control of chemical hazards. Personnel who work in cleanroom must practice contamination control measures through use of attire to trap contaminants being released from the body (gown, masks, coverall etc.) and *via* exposure to special rooms with airlocks and air showers.

Due to increasing interest in nanoparticle-based synthesis and manufacturing, the demand for access to cleanroom facilities has increased in both high and mid to low income countries, with larger number of staff working in confined spaces. As a result there is a need to monitor indoor air quality, especially to detect low levels of CO_2, which can have a substantial influence on the physical and mental health of an individual [3–6]. This will not only impact the quality of work produced by the personal, but it can develop into a significant health and safety risk for the life of the cleanroom worker (if the person faints to due to high CO_2 levels in the room), or upon exposure to hazardous chemicals used in the cleaning and manufacturing processes. Additionally, in the cleanroom several other gases (such as nitrogen and argon) and fumes from volatile solvents (such as acetone, isopropanol) are routinely present which may lead to increase in CO_2 content or interfere with the detection of CO_2 [5, 7–9].

Given the requirement for high sensitivity and selectivity, it is challenging to develop cleanroom-based CO_2 sensors which can specifically detect low CO_2 levels, for instance <500 ppm, in the presence of potential interferes [10]. While this problem is slowly being met by several advanced CO_2 sensors, significant challenge remains to develop a low-cost CO_2 detection technology with features that facilitate scalability from laboratory to mass-manufacture [11, 12]. Within these works, Kanaparthi *et al.* [10] introduces a new approach using a resistive gas sensor, based on ZnO nanoflakes, demonstrating excellent sensitivity and ultra-fast response (< 20 s) when exposed to 200-1025 ppm CO_2 at 250° C with the lowest detection limit of 200 ppm. In another work, chemiresistive sensor was also developed by Hannon *et al.* [13] using oxidized multi-walled carbon nanotubes (MWCNT) combined with iron oxide nanoparticles for detecting CO_2 at room temperature [14]. The addition of a small quantity of iron oxide nanoparticles significantly improved the sensitivity to CO_2 by approximately 5 times. This modification also extended the detection range from 100 ppm to 6000 ppm, while maintaining rapid response and recovery times of 10 s. The sensor exhibited good repeatability and reproducibility between measurements and different sensors.

In another work, there was a sensor created by S. Keerthana *et al.* by applying a hydrothermally prepared graphene oxide/cupric oxide nanocomposite onto a glass substrate using a spin coating technique [14]. Furthermore, the sensor exhibited a rapid response time of 25 s and a short recovery time of 8 seconds when exposed to varying concentrations of CO_2 gas ranging from 250 to 750 ppm. A sensor based on the organic compounds has also demonstrated good regeneration and reproducibility during recurrent usage, indicated by low relative standard deviation (RSD) values in the range of 0.174%–1.698% [15]. This sensing device shows LOD value around 250 ppm. In another example, a CO_2 sensor, γ-CD-MOF@RhB, was developed by Chen *et al.* based on a CO_2-switchable H^+/OH^- ion channel inspired by SLAC1 in plant cells [16]. The sensor shows excellent sensitivity (R_s/R_0 = 1.50, 100 ppm), selectivity, stability (5% reduction in 30 days), and 99.96% consistency with commercial infrared CO_2 meters.

Moreover, according to the Global monitoring laboratory [17] current level of CO_2 in the atmosphere is around 420 ppm. Numerous reasons might cause CO_2 levels in clean room laboratories to increase. This rise is partly caused by human activities, including the natural exhale of carbon dioxide. Furthermore, CO_2 may be released as a by-product during the operation of machinery that generates heat or combustion processes in clean rooms. Even with strict safeguards in place, small leaks or ambient air infiltration can occur in certain clean rooms, releasing outside CO_2. Furthermore, CO_2 may be a by-product of several chemical reactions carried out in clean rooms. Using ventilation and air purification systems that constantly monitor and control CO_2 levels and other impurities is essential to maintaining the strict air quality standards in clean rooms. Ensuring that clean room facilities maintain the necessary environmental conditions requires careful planning, execution, and upkeep of these systems. Some of the CO_2 sensors available in the market are provided in table S1.

Within this context, we have developed a cobalt nickel oxide ($CoNiO_2$) based nanoparticle-based CO_2 sensor (limit of detection < 20 ppm with certain reducing agent) using a simple solution combustion method. This method is based on a high temperature self-sustained reaction initiated in aqueous form to generate nanomaterials in powered form at large scale. The presence of a reducing agent generates specific properties within the resultant product. For instance, in this work, a solution of cobalt and nickel salts is mixed with a variety of reducing agents to produce $CoNiO_2$, where the choice of reducing agent may determine the morphological and physicochemical attributes of engineered nanomaterials. Esentially, we aim to understand how choice of reducing agent (citric acid, glycine, urea or glucose) dictates the performance of $CoNiO_2$ nanoparticles towards chemiresistive CO_2 detection, with respect to the 3 essential S's (sensitivity, selectivity and stability) and 5 essential R's (room temperature operation, range of detection, repeatability, response and recovery time, reproducibility). With respect to the intended application in cleanrooms, CO_2 sensing has been critically analyzed in the presence of common interfering analytes.

2. Methods

2.1. Chemicals and Reagents

For the fabrication of $CoNiO_2$ nanostructures, analytical grade chemicals with high purity were sourced from Sigma Aldrich, including Cobalt nitrate hexahydrate ($Co(NO)_2 \cdot 6H_2O$) (99.99%), Nickel nitratehexahydrate ($Ni(NO)_2 \cdot 6H_2O$) (99.99%), citric acid, glycine, urea and glucose. Deionized water with resistivity higher than 18.2 MΩ/cm was used to prepare all solutions.

2.2. Nanoparticle synthesis

The $CoNiO_2$ nanostructures were first fabricated by an solution combustion method [18] using stoichiometric variations of nickel and cobalt nitrate with selected reducing agents as listed in table 1.

Table 1. Reactant precursors and reaction conditions used for $CoNiO_2$ synthesis.

Reducing agent	Cobalt Nitrate (g)	Nickel Nitrate (g)	Reducing agent Quantity (g)	Temperature (˚C)	Duration (min)
Citric acid ($C_6H_8O_7$)	3.022	9.733	4.628	550	20
Glycine ($C_2H_5NO_2$)	3.022	9.733	3.657	550	20
Urea (CH_4N_2O)	3.022	9.733	4.380	550	20
Glucose ($C_6H_{12}O_6$)	3.022	9.733	3.290	550	20

During the fabrication, defined stoichiometric quantities of metal nitrates and reducing agent were added to a 500 ml glass beaker and dissolved using 100 ml of distilled water, prior to heating in a furnace at 550 ˚C for 2 h in N_2 environment. Initially, the solution started to boil leading to evaporation of water vapour resulting in formation of a viscous redox mixture gel. Due to high temperature, the gel underwent sudden flame combustion, which propagated throughout the mixture producing the $CoNiO_2$ product with the liberation of gases. The as produced product was further characterized for morphological and structural attributes through various characterizations.

2.3. Characterisation tools

The morphology, bonding configuration and crystal structure of the prepared nanostructures were systematically analyzed. Crystal structure was explored using a

Rigaku SmartLab X-ray diffractometer (XRD) having a Cu $k_{\alpha\ 1}$radiation source (3 kW) with wavelength of 1.540 Å. The morphology of the synthesized materials was examined using field-emission scanning electron microscope (FESEM-Base VI, AMETEK).

2.4. Device fabrication and experimental set-up

A glass substrate was first cleaned with a water and acetone solution to get rid of any impurities before being ready for $CoNiO_2$ deposition. $CoNiO_2$ was then dropped onto the substrate after being dissolved in ethanol. The solvent was then removed from the coated substrate by drying it at 60^{o}C, leaving a homogeneous layer of $CoNiO_2$. Note that the $CoNiO_2$ was dispersed in N, N-Methylpyrrolidone (NMP) using ultrasonication to allow NMP to bind on the nanoparticles to enhance the metal oxide's adhesion on glass. Previously, NMP has been used as a binder in printed electronic devices [19].

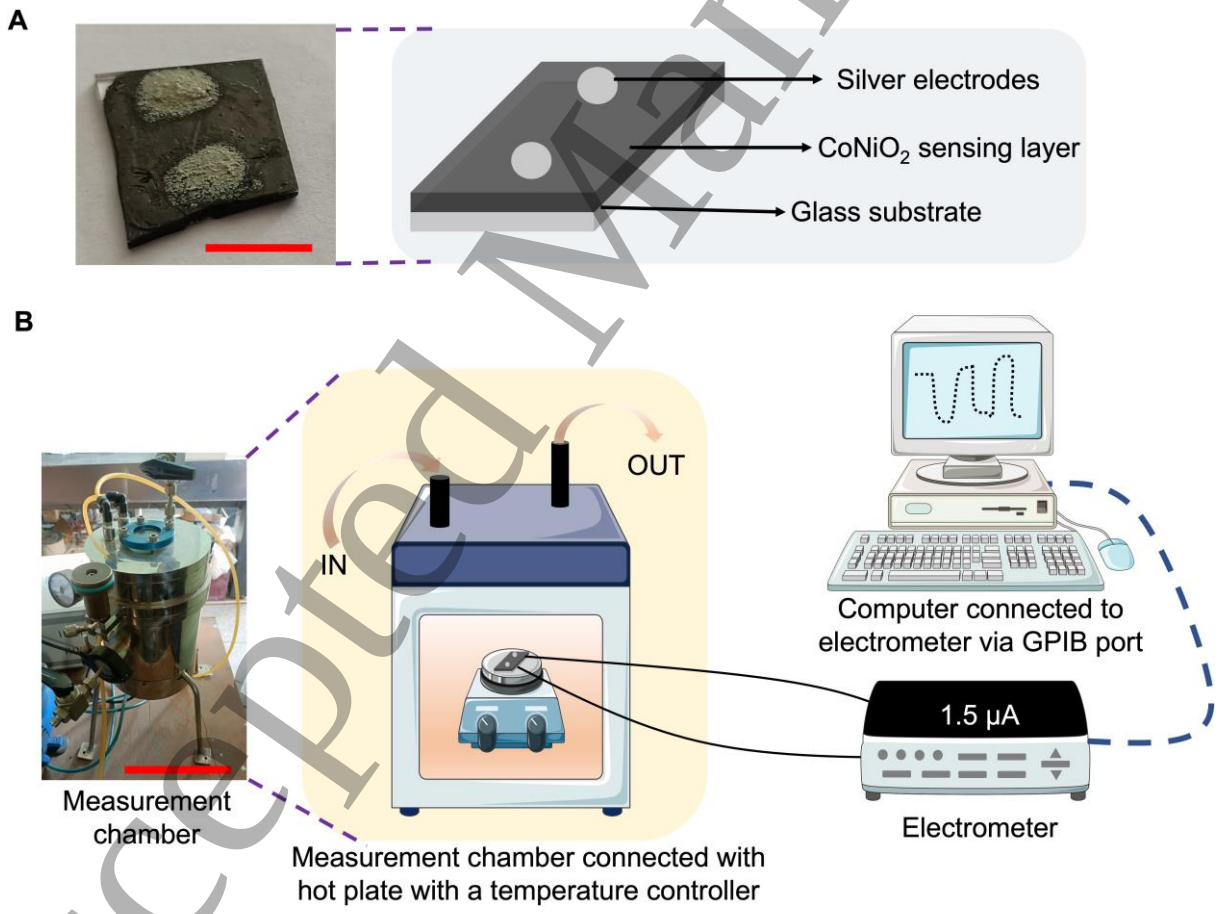

Figure 1. Sensing set-up for the evaluation of gas sensing performance. A) Schematic of the developed sensor and its corresponding architecture; B) Representation of the measurement set-up measurements are recorded using an electrometer connected to a computer via general purpose interface bus (GPIB) port. The scale bars in snapshots with A and B indicate lengths of 1 cm and 10 cm respectively.

The coated substrate was annealed at 250 ^{o}C for one hour in a furnace to increase

the stability and adherence of the deposition layer. The $CoNiO_2$ layer and the glass substrate were able to build robust chemical connections thanks to this heat treatment. The thickness of the $CoNiO_2$ layer was 8 μm. The substrate was further treated by applying silver electrodes to the surface after annealing. The distance between the electrodes was 5 mm. In order to assure adhesion and conductivity, the electrodes were then cured at 80°C. The $CoNiO_2$ coated glass substrate with silver electrodes was created in this last phase and is now ready for use in a range of applications. The CO_2 monitoring performances of prepared fabricated materials were evaluated from standard indigenously made automated sensing assessing apparatus (see Figure 1), comprised of a heater, a two-probe arrangement, and a temperature control device permitting observation of surface current as a function of temperature and concentration of CO_2. The change in surface current of sensing material was recorded through Keithley's electrometer. The concentration of CO_2 flow inside the sensing chamber was controlled through a mass-flow controller (MFC) and a vacuum pump for evacuation. The MFC was connected with the CO_2 cylinder. By using the MFC we control the flow of gas from 125-500 μL/min. We have injected the gas for 1 minute which allows us to vary the CO_2 gas inside the sensing set-up from 50-200 ppm. During the measurements, the stated concentration of a particular gas, such as 50 ppm, represents a ratio between the analyte and the gas, typically air (reference gas), present in the measurement environment.

3. Results and Discussion

3.1. Structural analysis

XRD data for the synthesized $CoNiO_2$ with respective reducing agents (citric acid, glycine, urea, and glucose) is shown in Figure 2i-iv. All prominent standard diffraction peaks conforming the formation of $CoNiO_2$ have been observed in recorded XRD spectra (JCPDS No. 10-0188) [20–22]. Diffraction peaks at 37°, 43°, and 63° are ascribed to (111), (200), and (220) planes of the $CoNiO_2$ phase, and a minor diffraction peak at around 45° can be indexed to the $NiCo_2O_4$ phase (JCPDS No. 20-0781) [23]. Amongst all, the sample prepared with urea (pattern ii) exhibits significantly broader peaks, indicating the presence of smaller nanoparticles/ nanostructures.

3.2. Morphological analysis

The morphology of as prepared $CoNiO_2$ nanostructures was examined using scanning electron microscope (SEM). At lower magnification, SEM micrographs reveal the presence of a porous network structure in all samples (Figure 2i-iv), with the corresponding high surface area being highly desirable for gas sensing applications. The formation of well-defined nanoparticles with sizes ranging between 50 nm to 200 nm was observed in urea mediated synthesis, Figure 2ii. This observation concurs with the XRD data demonstrating presence of highly crystalline small particles. It is well-known that nanomaterials with high specific surface area and networked structures exhibit good

performance in gas sensing applications. Consequently, the structural and morphological outcomes of prepared $CoNiO_2$ nanostructures strongly suggest their potential gas/vapor

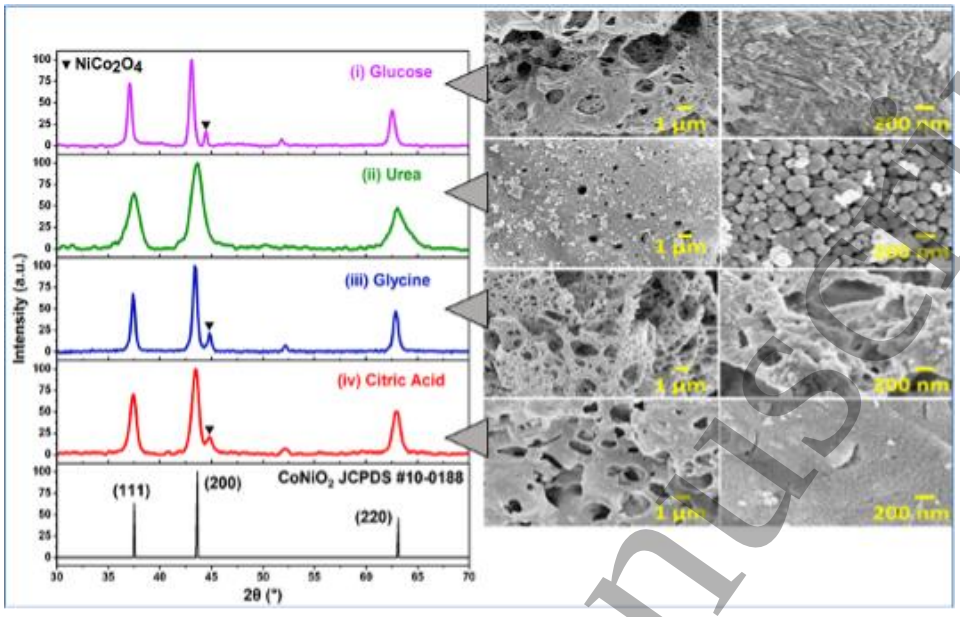

Figure 2. Structural and morphological evaluation of $CoNiO_2$ nanostructures. X-ray diffraction (XRD) micrograph and scanning electron microscope (SEM) images of $CoNiO_2$ nanostructures prepared by solution combustion method using (i) Glucose, (ii) Urea, (iii) Glycine and (iv) Citric Acid as reducing agents.

sensing applications, where it could be hypothesized that the urea based sample would perform with high sensitivity.

3.3. CO_2 monitoring performance

The CO_2 sensing behavior of fabricated nanostructures $CoNiO_2$ was assessed through consecutive cycles of CO_2 exposure. The current-time dependent variations under the ambient atmosphere and upon CO_2 exposure were recorded for the prepared samples with CO_2 ranging from 50-200 ppm, see Figure 3A i-iv. The variation in sensor current was measured in presence of CO_2 with respect to that in ambient conditions defined as the sensor response Equation (1) [24]:

$$Sensor\ response = \frac{I_{air}}{I_{co_2}} \quad (1)$$

Amongst the prepared samples, urea mediated $CoNiO_2$ nanoparticles exhibited the highest sensor response towards different concentrations of gaseous CO_2 (50-200 ppm), with around 22.22 for 200 ppm of CO_2. This can be ascribed to the smaller particle size, and the porous and connected networked structure of urea mediated $CoNiO_2$ nanoparticles compared to others, as supported by XRD and SEM analysis. Moreover, the sensing response was found to rapidly increase with rise in CO_2 concentration for all samples, which is attributed to larger probability of interaction between CO_2 molecules and sensor surface at higher concentrations. Sensors based on citric acid, glycine and glucose mediated $NiCoO_2$ showed significant sensor response of 6.5, 8.1 and 17.1 respectively at 200 ppm of CO_2.

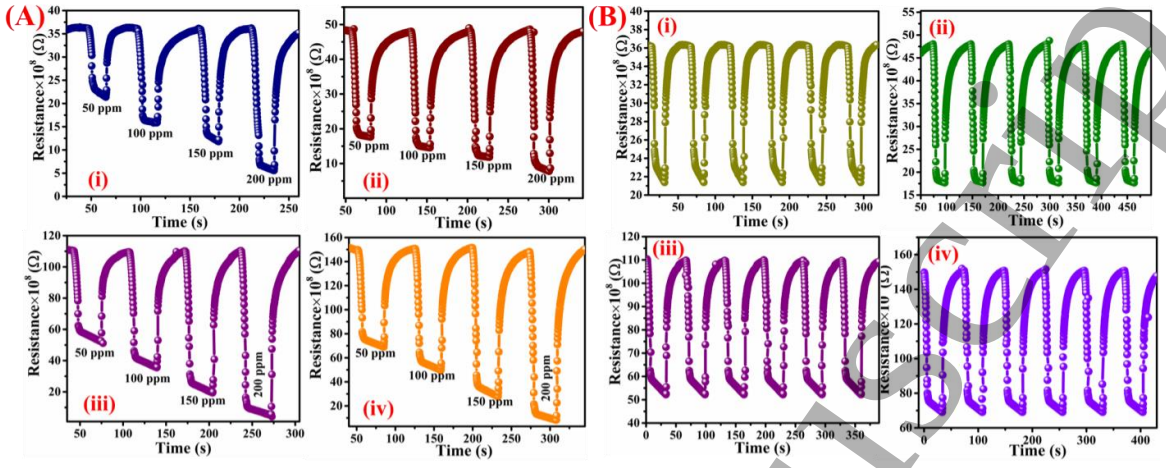

Figure 3. Real-time CO_2 detection. (A) Time dependent sensing properties of $NiCoO_2$ synthesized using various reducing agents (i) Citric acid (ii) Glycine (iii) Urea (iv) Glucose at different concentrations,and (B): Repeatability and stability of $NiCoO_2$nanostructures prepared by using (i) Citric acid (ii) Glycine (iii) Urea (iv)Glucose when exposed to 50 ppm CO_2 and at room temperature.

Another important commercial parameter of a bio/chemical sensor is defined in terms of repeatability, which essentially refers to the ability of a sensor to provide the same results under the same circumstances repeatedly. All the devices exhibited excellent reproducibility as function of time, Figure 3 (i-iv). To aid in the evaluation of device stability, the standard deviation (SD) can be used to estimate the variation in response upon exposure to the same conditions. From Figure 4 (i-iv), the SD of each device was calculated as 0.18, 0.31, 0.11 and 0.21 for the citric acid, glycine, urea and glucose mediated systems, respectively (using 5 replicates, also presented by error bars in Figure 4). The least SD for urea mediated synthesis may be attributed to the regular structures of the $NiCoO_2$ structures. The response of all sensor devices was observed to linearly increase with CO_2 concentration which is highly desirable for commercial prospects.

Device sensitivity was further critically analyzed through correlation between concentration, sensor response, the limit of detection (LOD) and limit of quantification (LOQ) (Equations (2) and (3)) [25–27]. The lowest amount of analyte in a sample that can be detected is it's called LOD, and the lowest amount that can be quantitatively identified under specified experimental conditions with declared acceptable precision and accuracy is called LOQ.

$$LOD = \frac{3.3 \times SD}{m} \quad (2)$$

$$LOQ = \frac{10 \times SD}{m} \quad (3)$$

Where, SD is the standard deviation of responses and m is the slope of the fitted straight line. The LOD for the urea-mediated sensor was determined to be 8.58 ppm, lowest of

the sensors produced, which is the lowest among all prepared devices. The LOD for citric acid, glycine and glucose mediated synthesized material was found to be 19.17, 11.14 and 9.40 ppm, respectivelyFigure 4v. LOQ values (Figure 4vi.), also confirmed urea-based materials to provide optimal performance (LOQ of 26.0 ppm, whereas for citric acid, glycine and glucose-based material g the LOQ values were 58.10, 33.76, and 28.49 ppm, respectively. Again, performance can be attributed to the optimal nanoparticle structure and morphology determined through characterization.

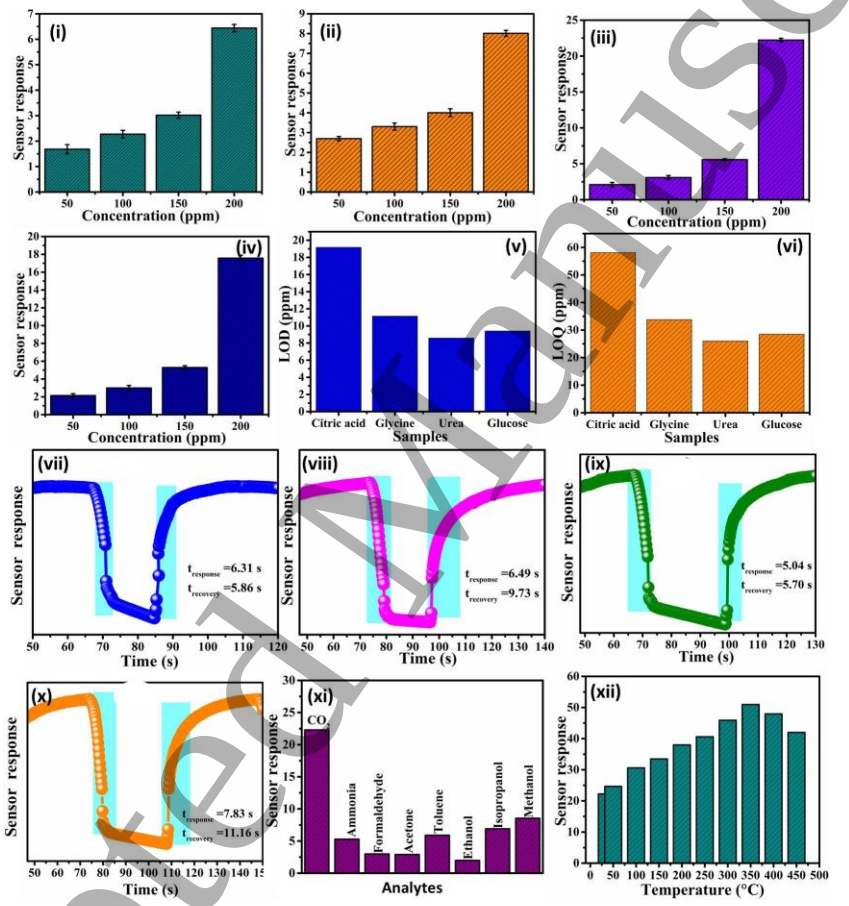

Figure 4. Sensing features of CO_2 sensor. Sensor response to increasing CO_2 levels for samples synthesized *via* (i) Citric acid (ii) Glycine (iii) Urea (iv) Glucose precursors. (v) LOD, and (vi) LOQ for respective devices. Response and recovery times for $CoNiO_2$ synthesized by usingthe fuel (vii) Citric acid (viii) Glycine (ix) Urea (x) Glucose, respectively; (xi) shows selectivity of the sample synthesized using urea; and (xii) shows the temperature dependence of the sensor response of same sample.

Response time is a key parameter for many sensing application, coupled to the time for a sensor to return to baseline value after the removal of the measured variable. The exponential rise and decay curves (equations 8 and 9) fitted between 10% and 90% and 90% to 10%, respectively, were used to estimate the sensor response and recovery times Figure 4vii-x. Rapid response and recovery times were observed for the sensor consisting of nanoparticles prepared *via* urea mediated synthesized, 5.04 s and 5.70 s, respectively. Devices build upon systems derived from citric acid, glycine and glucose

reducing agents gave response times of 6.31 s, 6.49 s and 7.83 s, respectively.

$$I(t) = I_{air} \cdot e^{-t/\tau_{response}} \quad (4)$$

$$I(t) = I_{air} \cdot 1 - e^{-t/\tau_{recovery}} \quad (5)$$

Given the performance of the urea mediated $CoNiO_2$ nanoparticles, sensing performance was further analyzed as function of temperature (Figure 4xi). In general, most semiconducting materials exhibit a strong sensor response at elevated temperature where the rate of surface adsorption is increased. In addition, in metal oxide based systems free electrons flow across the grain boundaries is enhanced when sensor materials are heated, typically to about 400 ˚C [28–30]. In this context, the highest sensor response recorded (50.94) was attained at 350 ˚C (Figure 4xi), with a decline in response observed above this temperature. On further raising the working temperature, the sensor response was observed to decline. For instance, at 400 ˚C, the sensor response was recorded to be around 47.95, and at 500 ˚C, it continues to fall to 41.97 (Figure 4xi). This effect is ascribed to increased oxygen adsorption above 350 ˚C saturating the system. This becomes saturated after the percolation value resulting in decrease of sensing response as function of temperature. The adsorbed oxygen's strong electron draws free electrons from inside the metal oxide, creating a potential barrier at the grain boundaries. By obstructing electron passage, this potential barrier raises the sensor resistance in pure air. However, the ideal temperature depends on the sensor's material and can be specific to the gases being detected with a crucial role played by the strength of the van der Walls forces between the material and the gas [31].

Reducing the working temperature to ambient conditions has significant benefit with respect to energy-efficiency, cost-effectiveness and simplicity of sensor architecture/ design. In this context, at room temperature, the urea-based nanoparticle sensor was shown to have a response of 22.22, demonstrating the strong gas adsorption/ desorption properties. It strongly suggests the fabricated sensor can be operated at room temperature and is economical in terms of power consumption and simple architect.

Sensor selectivity refers to the capacity to distinguish between the target and interfering molecules with specific sensor response to the target [32]. To evaluate the selectivity of the $CoNiO_2$ based sensors for application in cleanroom environments, the sensor response was recorded for the several VOCs including ammonia, formaldehyde, acetone, toluene, ethanol, isopropanol and methanol (Figure 4xii). In the presence of each of the above VOCs a strong sensor response of around 22.29 was obtained for 200 ppm of CO_2 (Figure 4xii). The reason for this selectivity can be ascribed to interaction and adsorption energies of this particular analyte with sensor surface [33]. Moreover, the signal arising from the various analytes can be distinguished from CO_2 using simple electronics on basis of their chemical nature (reducing/oxidizing analytes). Understanding and optimizing systems can further increase the selectivity of target analytes in presence of other interfering analytes such as alcohols and ammonia [25, 33–35].

The material exhibits reasonably high impedance, with values ranging from 132.27 MΩ to 135.98 MΩ, at lower humidity levels (10-25%RH) such as presented in Figure 5a. The impedance reduces as humidity levels rise to 35% and higher, with values ranging from 126.37 MΩ to 117.29 MΩ at 45% to 90% RH. This implies that at greater humidity levels, the material can be more vulnerable to moisture damage. The sensor response to CO_2 gas as also shown inFigure 5b, and it appears to be decreasing as humidity levels rise. At 10% RH, the highest response is recorded at 24.9, while at 90% RH; the lowest response is recorded at 19.5. This shows that moisture in the environment can impede the sensor's capacity to accurately detect CO_2 gas. Overall, there is not too much change in the sensor response as the %RH changes.

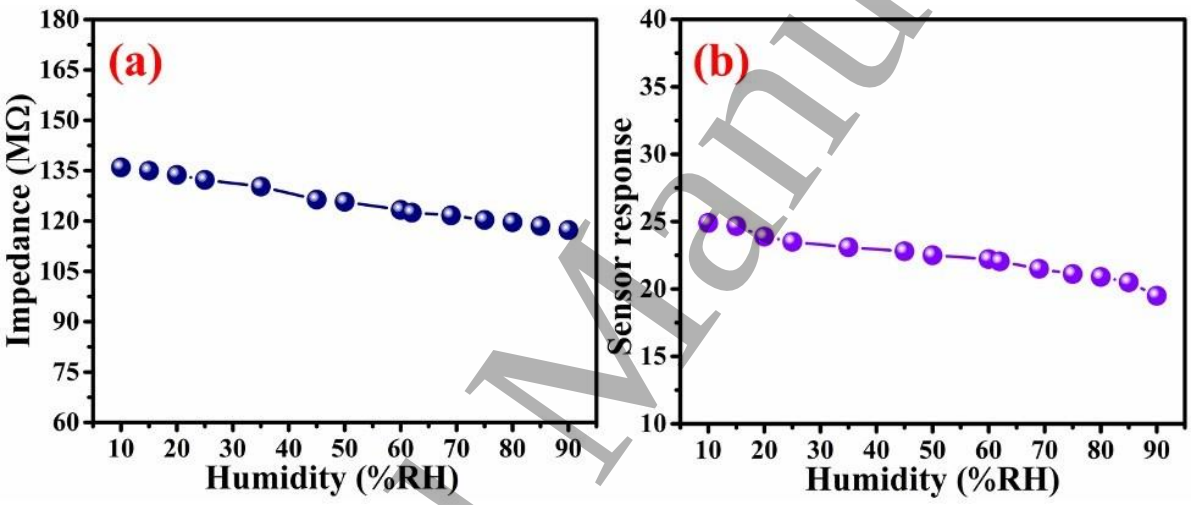

Figure 5. Sensor characteristics. (a) Change in the impedance with respect to humidity (b) Sensor response of the device withrespect to change in humidity at the room temperature and for 200 ppm of CO_2.

3.4. Sensing mechanism

A model of conduction in p-type oxide semiconductors is shown in Figure 6 where the rivalry between parallel pathways that traverse the resistive core (R_{core}) and along the narrow, p-semiconducting shell (R_{shell}) regions are depicted. If we consider the p-type material-based sensor, oxygen molecules can be adsorbed onto the active sites of $CoNiO_2$ surface, releasing holes which result in the production of chemisorbed oxygen species (Equations (6), (8) and (7)) [36]. This procedure may also cause the $CoNiO_2$ surface to develop an accumulation layer. According to Equation (9) , CO_2 molecules in the environment have also been seen to adsorb onto the active sites of a $CoNiO_2$ surface, releasing holes to sensing materials to generate $CO_3^{2-\cdot}$ Additional holes can then be released into $NiCoO_2$ by the adsorption CO_3^{2-} interacting with the adsorbed oxygen species in accordance with Equation (9) [36]. As a result of these processes, the $CoNiO_2$ surface collection layer becomes thicker, and the resistance decreases. The concept of adsorption/desorption typically serves as an explanation for the metal oxides gas sensing

technique. Due to the interaction of the targeted gas, the sensor film electrical resistance changes depending on whether it is oxidizing or reducing [37]. In the case of $CoNiO_2$, the response is generated as a result of chemisorption of CO_2 on the surface, primarily resulting from the NiO element of the nanostructure with the Co acting as a sensitization layer altering the carrier density in the NiO layer [38]. Electrical resistance typically rises for n-type semiconductors in an oxidizing gas atmosphere, such as CO_2 and NO_2, and falls in the presence of reducing gas atmospheres, while p-type semiconductors exhibit the reverse tendency. The creation of oxygen species such O_2^-, O^-, and O^{2-}, which can be characterized as the following processes (Equations (6), (7) and (8)), occurs when atmospheric oxygen adsorbed on the surface of the material device before the introduction of CO_2 attracts electrons from the conduction band [10, 39]. Due to the production of oxygen species on the sensing surface, an electronic depletion layer and depletion region is generated. This region serves as a potential barrier to charge carrier transfer. After the adsorption is saturated, the sensor resistance typically increases and remains constant. Due to the oxidizing nature of CO_2 and the formation of metastable (CO_3^{2-}) complexes on the surface of the film, electrons are transferred to the CO_2 molecule specifically when it combines with those oxygen species[19]. Due to the decreasing free electron density and escalating depletion, the creation of CO_3^{2-} complexes decreases the conductivity of the sensor film. Thus, depending on the CO_2 content, the resistance of the film quickly rises [40]. When the flow of CO_2 is stopped, the CO_3^{2-}complexes decompose into CO_2, and trapped electrons are released onto the sensor film, bringing the resistance of the film down to its initial value.

$$O_{2(gas)} \rightarrow O_{2(ads)} \tag{6}$$

$$O_{2(gas)} + e^-(CB) \rightarrow O^-_{2(ads)} \tag{7}$$

$$O^-_{2(gas)} + e^-(CB) \rightarrow 2O^-_{(ads)} \tag{8}$$

$$2CO_2 + O_2^- + e^- \rightarrow 2CO_3^{2-} \tag{9}$$

4. Conclusions

This work reports a low cost strategy to develop $CoNiO_2$ nanoparticle-based chemiresistive gas sensors *via* a facile solution combustion method. Various reducing agents (citric acid, glycine, urea and glucose) were shown to direct the architecture of the engineered $CoNiO_2$ nanoparticles. Urea mediated synthesis generated $CoNiO_2$ nanoparticles with high crystallinity, high porosity and uniformity in size distribution. The fabricated $CoNiO_2$ nanoparticle-based sensors were evaluated for

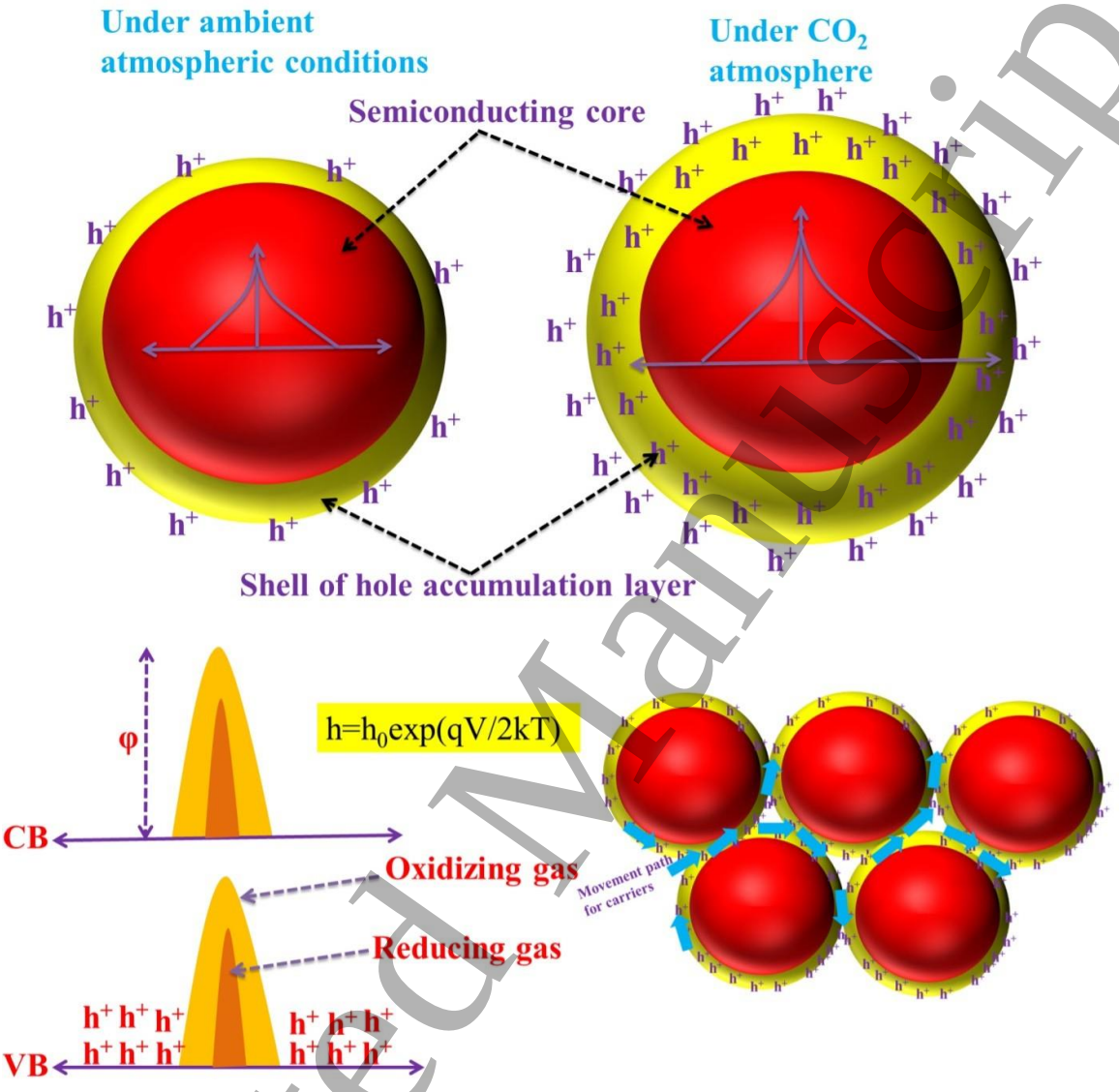

Figure 6. Gas sensing mechanism. Schematic representation of the sensing mechanismfor the p-type sensing layer under ambient atmospheric and upon exposure to CO_2.

CO_2 sensing in terms of selectivity, sensitivity and stability, with urea based nanoparticles exhibiting high-performance towards low concentrations of CO_2 (as low as 200 ppm) when compared to particles produced by other reducing agents. Moreover, the sensor demonstrated high selectivity in presence of prominent interfering analytes (ammonia, formaldehyde, acetone, toluene, ethanol, isopropanol and methanol) commonly present in cleanroom facilities. The sensor also exhibited ambient stability, room temperature operation, high repeatability, prompt response and recovery rates, and good reproducibility suggesting demonstrating significant potential for the intended application of cleanroom CO_2 level monitoring. These results open a new window to guide future research dedicated to developing routine cleanroom sensors with high-

performance in monitoring diversified in-room analytes.

Acknowledgment

The author (CM) is grateful to the Management, Rashtreeya Sikshana Samithi Trust, and the Principal, RV College of Engineering for constant support and encouragement. This study was supported by Rashtreeya Sikshana Samithi Trust (RSST) Bengaluru, India under RVCE sustainability fund (Seed money grant no:RVE/A/c/116/2021-22/ Dated 08 July 2021). Nikhil Bhalla and Vishal Chaudhary would also like to thank support from the Industry-Academia Collaborative Grant from British Council-Going Global Partnership Program for facilitation of the joint collaboration.

References

[1] Yang Z, Hao Y, Shi W, Shao X, Dong X, Cheng X, Li X and Ma X 2021 *Journal of Building Engineering* **42** 103083–103083

[2] Ruberti M 2023 *Science of The Total Environment* **858** 159873–159873

[3] Chaudhary V, Ashraf N, Khalid M, Walvekar R, Yang Y, Kaushik A and Mishra Y K 2022 *Advanced Functional Materials* **32** 2112913–2112913

[4] Chaudhary V, Gautam A, Silotia P, Malik S, Hansen R D O, Khalid M, Khosla A, Kaushik A and Mishra Y K 2022 *Materials Today* **60** 201–226

[5] Davey A K, Gao X, Xia Y, Li Z, Dods M N, Delacruz S, Pan A, Swamy S, Gardner D and Carraro C 2021 *Sensors and Actuators B: Chemical* **344** 130313–130313

[6] Escobedo P, Fernández-Ramos M D, López-Ruiz N, Moyano-Rodríguez O, Martínez-Olmos A, Vargas-Sansalvador I M P D, Carvajal M A, Capitán-Vallvey L F and Palma A J 2022 *Nature Communications* **13** 72–72

[7] Mata T M, Martins A A, Calheiros C S C, Villanueva F, Alonso-Cuevilla N P, Gabriel M F and Silva G V 2022 *Environments* **9** 118–118

[8] Chaudhary V, Awan H T A, Khalid M, Bhadola P, Tandon R and Khosla A 2022 *Sensors and Actuators B: Chemical* **379** 133225–133225

[9] Chaudhary V, Kaushik A, Furukawa H and Khosla A 2022 *ECS Sensors Plus* **1** 13601–13601

[10] Kanaparthi S and Singh S G 2019 *ACS Applied Nano Materials* **2** 700–706

[11] Dhahri R, Leonardi S G, Hjiri M, Mir L E, Bonavita A, Donato N, Iannazzo D and Neri G 2017 *Sensors and Actuators B: Chemical* **239** 36–44

[12] Vafaei M and Amini A 2021 *ACS Sensors* **6** 1536–1542

[13] Hannon A and Li J 2019 *Sensors* **19** 3848

[14] Keerthana S and Rathnakannan K 2021 *Journal of Materials Science: Materials in Electronics* **32** 23513–23521

[15] Daud A I, Wahid K A A and Khairul W M 2019 *Organic Electronics* **70** 32–41

[16] Chen H, Lu R, Gao Y, Yue X, Yang H, Li H, Lee Y K, French P J, Wang Y and Zhou G 2023 *Journal of Materials Chemistry A* **11** 21959–21971

[17] Trends in Atmospheric Carbon Dioxide URL https://gml.noaa.gov/ccgg/trends/

[18] Qin M, Liang H, Zhao X and Wu H 2020 *Ceramics International* **46** 22313–22320

[19] Dai J, Ogbeide O, Macadam N, Sun Q, Yu W, Li Y, Su B L, Hasan T, Huang X and Huang W 2020 *Chemical Society Reviews* **49** 1756–1789

[20] Chen S, Liang J, Pang Y, Dong B, Xu X and Ding S 2018 *ChemPlusChem* **83** 929–933

[21] Xu X, Dong B, Ding S, Xiao C and Yu D 2014

[22] Zhang J, Chen Z, Wang Y, Yan X, Zhou Z and Lv H 2019 *Nanoscale Research Letters* **14** 1–11

[23] Khalid S, Cao C, Ahmad A, Wang L, Tanveer M, Aslam I, Tahir M, Idrees F and Zhu Y 2015

[24] Yadav P, Singh A, Singh S and Kumar D 2022 *ECS Sensors Plus* **1** 42601–42601

[25] Chaudhary V, Channegowda M, Ansari S A, Rajan H K, Kaushik A, Khanna V, Zhao Z, Furukawa H and Khosla A 2022 *Journal of Materials Research and Technology* **20** 2468–2478

[26] Fatima Z, Gautam C, Singh A, Avinashi S K, Yadav B C and Khan A A 2022 *Journal of Materials Science: Materials in Electronics* **33** 1192–1210

[27] Rajesh N, Kannan J C, Krishnakumar T, Bonavita A, Leonardi S G and Neri G 2015 *Ceramics International* **41** 14766–14772

[28] Chaudhary P, Verma A, Mishra A, Yadav D, Pal K, Yadav B C, Kumar E R, Thapa K B, Mishra S and Dwivedi D K 2022 *Physica E: Low-dimensional Systems and Nanostructures* **139** 115174–115174

[29] Chaudhary V 2021 *Applied Physics A* **127** 536–536

[30] Singh A, Verma A and Yadav B C 2022 *ECS Sensors Plus* **1** 25201–25201

[31] Bharathi P, Harish S, Mathankumar G, Mohan M K, Archana J, Kamalakannan S, Prakash M, Shimomura M and Navaneethan M 2022 *Applied Surface Science* **600** 154086–154086

[32] Wusiman M and Taghipour F 2022 *Critical Reviews in Solid State and Materials Sciences* **47** 416–435

[33] Chaudhary V 2022 *Polymer-Plastics Technology and Materials* **61** 107–115

[34] Chaudhary V and Kaur A 2015 *RSC Advances* **5** 73535–73544

[35] Chaudhary V and Chavali M 2021 *Journal of Applied Polymer Science* **138** 51288–51288

[36] Moumen A, Kumarage G C W and Comini E 2022 *Sensors* **22** 1359–1359

[37] Kim H J and Lee J H 2014 *Sensors and Actuators B: Chemical* **192** 607–627

[38] Iwata T, Matsuda K, Takahashi K and Sawada K 2017 *CO2 sensing characteristics of a La2O3/SnO2 stacked structure with micromachined hotplates* **17** 2156–2156

[39] Zhang C, Xu K, Liu K, Xu J and Zheng Z 2022 *Coordination Chemistry Reviews* **472** 214758–214758

[40] Franke M E, Koplin T J and Simon U 2006 *small* **2** 36–50